

Supplementary File

A modeling approach for assessing ecological risks of neonicotinoid insecticides from emission to non-target organisms: A case study of cotton plant

Zijian Li^{a*}, Minmin Li^b, Shan Niu^c

^a School of Public Health (Shenzhen), Sun Yat-sen University, Shenzhen, Guangdong, 518107, China.

^b Key Laboratory of Agro-products Quality and Safety Control in Storage and Transport Process, Chinese Academy of Agricultural Sciences, Beijing 100000, China.

^c Department of Civil & Environmental Engineering, University of Pittsburgh, Pittsburgh, PA 15260, United States.

*Corresponding information: ORCID: 0000-0002-9291-5966; Phone: +86 136 4430 2865;

Email: lizijian3@mail.sysu.edu.cn

14	Table of contents
15	S1. Plant uptake model
16	S2. Insecticide dissipation kinetics in soil
17	S3. Chemical-specific model inputs
18	S4. Variability analysis
19	S4.1 Soil properties
20	S4.2 Dissipation half-lives of insecticides in soil
21	S5. Supplementary figures
22	S6. Model refinement for site-specific assessment
23	S6.1 Weather input variables
24	S6.2 Exposure input variables
25	S6.3 Toxicological input variables
26	References

S1. Plant uptake model

The plant uptake model for simulating the residue in leaves, pollen, and nectar for the vegetative development and flowing stages was introduced by Li (2022). In this section, the main modeling processes associated with the input values specified for cotton plants are provided.

In the vegetative development stage, the modified one-compartment uptake model (Li, 2021; Trapp and Matthies, 1995), including the transpiration (i.e., residue uptake from soil) and surface deposition (i.e., residue uptake via penetration through leaf cuticle) uptake routes (Fantke et al., 2011), was applied to describe the uptake of neonicotinoid insecticides by cotton plants. The uptake process can be expressed in the following equations.

The residue fate in the leaf compartment:

$$\frac{dC_{Leaf}(t)}{dt} = k_{Up,Soil}C_{Soil}(t) + k_{Up,Surface}C_{Surface}(t) - (k_{El,Air} + k_{El,Degra} + k_{El,Grow})C_{Leaf}(t) \quad (s1)$$
$$\forall t \in [0, t_F)$$

where,

$C_{Leaf}(t)$ (mg kg⁻¹) is the residue level in the leaf as a function of time (t, d);

$C_{Soil}(t)$ (mg kg⁻¹) is the residue level in soil (surface) as a function of t;

$C_{Surface}(t)$ (mg kg⁻¹) is the residue level on the leaf surface as a function of t;

$k_{Up,Soil}$ (d⁻¹) is the uptake rate constant of the residue in the leaf via transpiration from soil water;

$k_{Up,Surface}$ (d⁻¹) is the uptake rate constant of the residue in the leaf via surface deposition;

$k_{El,Air}$ (d⁻¹) is the elimination rate constant of the residue in the leaf via volatilization;

44 $k_{El,Degra}$ (d^{-1}) is the elimination rate constant of the residue in the leaf via degradation, which was
 45 approximated using the dissipation half-life in plant matrix (i.e., RL50) (Lewis et al., 2016) due to
 46 the information limitation;

47 $k_{El,Grow}$ (d^{-1}) is the elimination rate constant of the residue in the leaf via dilution due to the plant
 48 growth;

49 “ $t = 0$ ” denotes the time when insecticide application occurs;

50 t_F (d) denotes the time when the cotton plant enters the flowering stage.

51 The residue fate in the soil compartment:

$$C_{Soil}(t) = C_{Soil}(0) \exp(-k_{Diss,Soil}t) \quad \forall t \in [0, \infty] \quad (s2a)$$

$$C_{Soil}(0) = \frac{AR \times f_{Soil} \times cf_1}{\rho_{Soil} \times H_{Soil} \times cf_2} \quad (s2b)$$

52 where,

53 ρ_{Soil} ($kg L^{-1}$) is the bulk density of soil;

54 f_{Soil} (unitless) is the mass fraction of the residue in soil (initial distribution);

55 H_{Soil} (m) is the height of the surface soil;

56 cf is the unit conversion factor.

57 The residue fate in the leaf surface:

$$C_{Surface}(t) = C_{Surface}(0) \exp(-k_{Diss,Surface}t) \quad \forall t \in [0, t_H] \quad (s3a)$$

$$C_{Surface}(0) = \frac{AR \times f_{Surface} \times cf_1}{LAI \times LMA \times \frac{1}{1 - W_{Leaf}}} \quad (s3b)$$

58 where,

59 $k_{Diss, Surface}$ (d^{-1}) is the dissipation rate constant of the residue on the leaf surface, which can be
60 approximated as four times as the dissipation rate constant in soil (Juraske et al., 2008);
61 $f_{Surface}$ (unitless) is the mass fraction of the residue on the leaf surface (initial distribution);
62 LAI ($m^2 m^{-2}$) is the leaf area index of the cotton plant;
63 LMA ($kg m^{-2}$) is the leaf mass (dry) per area of the cotton plant;
64 W_{Leaf} ($g g^{-1}$) is the water content of the leaf.
65 Then, Eq. (1) can be solved with the initial condition “ $C_{Leaf}(0) = 0$ ” as follows:

$$\begin{aligned}
& C_{Leaf}(t) \\
&= \left(\frac{AR \times f_{Soil} \times cf_1}{\rho_{Soil} \times H_{Soil} \times cf_2} \right) \left(\frac{k_{Up, Soil}}{k_{EL, Air} + k_{EL, Degra} + k_{EL, Grow} - k_{Diss, Soil}} \right) \{ \exp(-k_{Diss, Soil} t) \\
&\quad - \exp[-(k_{EL, Air} + k_{EL, Degra} + k_{EL, Grow})t] \} \\
&\quad + \left(\frac{AR \times f_{Surface} \times cf_1}{LAI \times LMA \times \frac{1}{1 - W_{Leaf}}} \right) \left(\frac{k_{Up, Surface}}{k_{EL, Air} + k_{EL, Degra} + k_{EL, Grow} - k_{Diss, Surface}} \right) \{ \exp(-k_{Diss, Surface} t) \\
&\quad - \exp[-(k_{EL, Air} + k_{EL, Degra} + k_{EL, Grow})t] \} \forall t \in [0, t_F]
\end{aligned} \tag{s4}$$

66 In the flowering stage, the flower compartment was integrated into the plant uptake model, and
67 the simple partitioning method (i.e., the partitioning of the residue between pollen or nectar and
68 phloem sap) was applied to simulate the residue levels in pollen and nectar (Li, 2022), which can
69 be expressed as follows:

$$\frac{C_{Pollen}(t)}{C_{Phloem}(t)} = K_{P-Ph} \forall t \in [t_F, t_H] \tag{s5a}$$

$$\frac{C_{Nectar}(t)}{C_{Phloem}(t)} = K_{N-Ph} \forall t \in [t_F, t_H] \tag{s5b}$$

$$\frac{C_{Leaf}(t)}{C_{Phloem}(t)} = K_{L-Ph} \forall t \in [t_F, t_H] \tag{s5c}$$

70 where,

- 71 $C_{Pollen}(t)$ (mg kg⁻¹) is the residue level in pollen as a function of t;
- 72 $C_{Nectar}(t)$ (mg kg⁻¹) is the residue level in nectar as a function of t;
- 73 $C_{Pholem}(t)$ (mg L⁻¹) is the residue level in phloem sap as a function of t;
- 74 K_{P-Ph} (L kg⁻¹) is the partition coefficient of the residue between pollen and phloem sap;
- 75 K_{N-Ph} (L kg⁻¹) is the partition coefficient of the residue between nectar and phloem sap;
- 76 K_{L-Ph} (L kg⁻¹) is the partition coefficient of the residue between leaf and phloem sap;
- 77 t_H (d) is the time at harvest, which equals the preharvest interval (PHI, d) of the neonicotinoid
- 78 insecticide.
- 79 Therefore, RUDs of the neonicotinoid insecticide in pollen (RUD_{Pollen}) and nectar (RUD_{Nectar}) can be
- 80 expressed as follows:

$$\begin{aligned}
 & RUD_{Pollen}(t) \\
 &= \left(\frac{K_{P-L} \times f_{Soil} \times cf_1}{\rho_{Soil} \times H_{Soil} \times cf_2} \right) \left(\frac{k_{Up,Soil}}{k_{El,Air} + k_{El,Degra} + k_{El,Grow} - k_{Diss,Soil}} \right) \{ \exp(-k_{Diss,Soil}t) \\
 &\quad - \exp[-(k_{El,Air} + k_{El,Degra} + k_{El,Grow})t] \} \\
 &\quad + \left(\frac{K_{P-L} \times f_{Surface} \times cf_1}{LAI \times LMA \times \frac{1}{1 - W_{Leaf}}} \right) \left(\frac{k_{Up,Surface}}{k_{El,Air} + k_{El,Degra} + k_{El,Grow} - k_{Diss,Surface}} \right) \{ \exp(-k_{Diss,Surface}t) \\
 &\quad - \exp[-(k_{El,Air} + k_{El,Degra} + k_{El,Grow})t] \} \forall t \in [t_F, t_H]
 \end{aligned} \tag{s6a}$$

$$\begin{aligned}
 & RUD_{Nectar}(t) \\
 &= \left(\frac{K_{N-L} \times f_{Soil} \times cf_1}{\rho_{Soil} \times H_{Soil} \times cf_2} \right) \left(\frac{k_{Up,Soil}}{k_{El,Air} + k_{El,Degra} + k_{El,Grow} - k_{Diss,Soil}} \right) \{ \exp(-k_{Diss,Soil}t) \\
 &\quad - \exp[-(k_{El,Air} + k_{El,Degra} + k_{El,Grow})t] \} \\
 &\quad + \left(\frac{K_{N-L} \times f_{Surface} \times cf_1}{LAI \times LMA \times \frac{1}{1 - W_{Leaf}}} \right) \left(\frac{k_{Up,Surface}}{k_{El,Air} + k_{El,Degra} + k_{El,Grow} - k_{Diss,Surface}} \right) \{ \exp(-k_{Diss,Surface}t) \\
 &\quad - \exp[-(k_{El,Air} + k_{El,Degra} + k_{El,Grow})t] \} \forall t \in [t_F, t_H]
 \end{aligned} \tag{s6b}$$

81 where,

82 K_{P-L} (unitless) is the partition coefficient of the residue between pollen and leaf, which can be
83 calculated by dividing K_{P-ph} by K_{L-ph} ;

84 K_{N-L} (unitless) is the partition coefficient of the residue between nectar and leaf, which can be
85 calculated by dividing K_{N-ph} by K_{L-ph} .

86 Values of the non-chemical-specific model inputs are provided in Table S1. Calculation processes
87 of the residue-bioconcentration-related (leaf) rate constants are provided in the following equations.

88 For the uptake process via transpiration, $k_{Up,Soil}$ can be estimated using the transpiration rate of the
89 cotton plant and the transpiration stream conversion factor (Trapp and Matthies, 1995) as follows:

$$k_{Up,Soil} = \frac{Q_{Leaf} \times TSCF}{M_{Leaf} \times K_{SW}} \quad (s7)$$

90 where,

91 Q_{Leaf} ($L d^{-1}$) is the transpiration rate of the single leaf;

92 M_{Leaf} (kg) is the mass of a single leaf;

93 $TSCF$ (unitless) is the transpiration stream conversion factor;

94 K_{SW} ($L kg^{-1}$) is the partition coefficient of the residue between soil and water.

95 As the transpiration of plant leaves is dependent on the relative humidity and temperature of air,

96 Q_{Leaf} can be estimated using the weather-dependent model (Li, 2020) as follows:

$$Q_{Leaf}(T_A, RH_A) = \eta A_{Leaf} LAI \left[\frac{2.50 \times 10^6 (31.145 - 0.1T_A)}{(T_A - 35.85)^2} + 610.78 \left(1 - \frac{RH_A}{100} \right) \right] \exp \left[\frac{17.2(T_A - 273.15)}{T_A - 35.85} \right] \quad (s8)$$

97 where,

98 η ($\text{L m}^{-2}\text{d}^{-1}$) is the transpiration rate coefficient, calculated from the vapor pressure deficit and the
99 stomatal resistances (Li, 2020; Li and Niu, 2021);

100 A_{Leaf} (m^2) is the area of the single cotton leaf;

101 T_A (K) is the air temperature;

102 RH_A (%) is the relative humidity of air.

103 For a general estimate, the reference state (i.e., 298.15 K and 50 %) (Li and Niu, 2021) was applied
104 to calculate the Q_{Leaf} value.

105 For the uptake process via surface deposition, $k_{Up, Surface}$ can be estimated, using the residue
106 mobility in the leaf cuticle and the partitioning process of the residue between cuticle and water
107 (Fantke et al., 2011; Juraske et al., 2007) as follows:

$$k_{Up, Surface} = k_{Cuticle} K_{CW} \quad (\text{s9})$$

108 where,

109 $k_{Cuticle}$ (d^{-1}) is the rate constant of the residue mobility in the leaf cuticle, which can be estimated
110 using the molecular weight (MW, g mol^{-1}) (Fantke et al., 2011; Juraske et al., 2007);

111 K_{CW} (L L^{-1}) is the partition coefficient of the residue between leaf cuticle and water, which can be
112 estimated using the partition coefficient between octanol and water (K_{OW} , L L^{-1}) (Fantke et al.,
113 2011; Juraske et al., 2007).

114 For the elimination process via volatilization, $k_{EL, Air}$ can be estimated by modeling the one-side
115 residue exchange with the air (Trapp and Matthies, 1995) as follows:

$$k_{EL, Air} = \frac{g}{L_{Leaf} \rho_{Leaf} K_{LA}} \quad (\text{s10})$$

116 where,

117 g (m d^{-1}) is the gas conductance;

118 L_{Leaf} (m) is the leaf thickness;

119 ρ_{Leaf} (kg L^{-1}) is the fresh leaf density;

120 K_{LA} (L kg^{-1}) is the partition coefficient of the residue between leaf and air.

121 For the residue partitioning among plant tissues, the composition-based approach was applied to
122 approximate the partition coefficients (Chiou et al., 2001; Trapp et al., 2007), of which the general
123 formula can be expressed as follows:

$$K_{i-j} \approx \frac{1.22Lip_i(K_{OW})^{0.77} + Carb_iK_{ch} + \frac{W_i}{\rho_{Water}}}{1.22Lip_j(K_{OW})^{0.77} + Carb_jK_{ch} + \frac{W_j}{\rho_{Water}}} \quad (\text{s11})$$

124 where,

125 K_{i-j} (L kg^{-1}) is the partition coefficient of the residue between compartments i and j;

126 Lip (L kg^{-1}) is the lipid content;

127 $Carb$ (kg kg^{-1}) is the carbohydrate content;

128 K_{ch} (L kg^{-1}) is the partition coefficient of the residue between carbohydrate and water;

129 ρ_{Water} (kg L^{-1}) is the density of water.

130 For the residue partitioning between leaf and air, K_{LA} can be estimated according to the
131 composition of the leaf (Trapp, 2007) as follows:

$$K_{LW} = \frac{W_{Leaf}}{\rho_{Water}} + Lip_{Leaf} \times \frac{(K_{OW})^{0.95}}{\rho_{Octanol}} \quad (\text{s12a})$$

$$K_{LA} = \frac{K_{LW}}{K_{AW}} \quad (s12a)$$

132 where,

133 Lip_{Leaf} ($g\ g^{-1}$) is the lipid content of the leaf;

134 $\rho_{Octanol}$ ($kg\ L^{-1}$) is the density of octanol;

135 K_{LW} ($L\ kg^{-1}$) is the partition coefficient of the residue between leaf and water.

136 For the residue partitioning in soil environment, K_{SW} can be estimated according to the
 137 composition of soil (Paraíba and Kataguirí, 2008; Trapp et al., 2007) as follows:

$$K_{SW} = \frac{f_{OC} \times K_{OC} \times \rho_{Soil,dry} + f_{Water} + f_{Air} \times K_{AW}}{\rho_{Soil,wet}} \quad (s13)$$

138 where,

139 f_{OC} ($L\ L^{-1}$) is the organic matter volumetric fraction of soil;

140 f_{Water} ($L\ L^{-1}$) is the water volumetric fraction of soil;

141 f_{Air} ($L\ L^{-1}$) is the air volumetric fraction of soil;

142 K_{AW} ($L\ L^{-1}$) is the partition coefficient of the residue between air and water;

143 K_{OC} ($L\ kg^{-1}$) is the partition coefficient of the residue between organic matter and water;

144 $\rho_{Soil,dry}$ ($kg\ L^{-1}$) is the density of dry soil;

145 $\rho_{Soil,wet}$ ($kg\ L^{-1}$) is the density of wet soil;

146 Values of the model inputs are provided in Table S1.

147 Table S1. Summary of inputs of the plant uptake model.

Variables	Variables	Units	Values	References
Bulk density of soil (wet)	ρ_{Soil}	$\text{kg}\cdot\text{L}^{-1}$	1.5	Generic
Depth of surface soil	H_{Soil}	m	0.05	Default
Area of a single leaf	A_{Leaf}	m^2	0.01	Estimated (Mukherjee et al., 2015).
Mass of a single leaf	M_{Leaf}	kg	8×10^{-4}	Estimated using the leaf area of 0.01 m^2 (Mukherjee et al., 2015).
Transpiration rate coefficient	η	$\text{L}\cdot\text{m}^{-2}\text{d}^{-1}$	0.0025	(Li, 2020; Li and Niu, 2021)
Leaf area index	LAI	$\text{m}^2\cdot\text{m}^{-2}$	3.0	Estimated for 50 days after germination (Monteiro et al., 2006).
Leaf mass (dry) per area	LMA	$\text{kg}\cdot\text{m}^{-2}$	0.1	Estimated (Meng et al., 2021).
Thickness of leaf	L_{Leaf}	m	0.0002	Estimated (Meng et al., 2021).
Mass fraction of residues on soil after application	f_{Soil}	unitless	0.223	Estimated based on the capture coefficient of 0.5 and LAI of $3.0 \text{ m}^2\cdot\text{m}^{-2}$ (Fantke et al., 2011; Juraske et al., 2007).
Mass fraction of residues on leaf surfaces after application	$f_{Surface}$	unitless	0.612	Estimated based on the fraction of the loss to air of 16.5% and f_{Soil} (Fantke et al., 2011; Juraske et al., 2007).
Water content of leaf	W_{Leaf}	$\text{kg}\cdot\text{kg}^{-1}$	0.8	Default
Lipid content of leaf	Lip_{Leaf}	$\text{kg}\cdot\text{kg}^{-1}$	0.02	Default (Trapp and Matthies, 1995)
Carbohydrate content of leaf	$Carb_{Leaf}$	$\text{kg}\cdot\text{kg}^{-1}$	0.1	Default (Wilson and Mannetje, 1978)
Water content of nectar	W_{Nectar}	$\text{kg}\cdot\text{kg}^{-1}$	0.7	Default
Lipid content of nectar	Lip_{Nectar}	$\text{kg}\cdot\text{kg}^{-1}$	0.0	Default
Carbohydrate content of nectar	$Carb_{Nectar}$	$\text{kg}\cdot\text{kg}^{-1}$	0.3	Default
Water content of pollen	W_{Pollen}	$\text{kg}\cdot\text{kg}^{-1}$	0.13	Estimated (Human and Nicolson, 2006)
Lipid content of pollen	Lip_{Pollen}	$\text{kg}\cdot\text{kg}^{-1}$	0.087	Estimated by converting from the dry mass fraction of 0.1 (Human and Nicolson, 2006).
Carbohydrate content of pollen	$Carb_{Pollen}$	$\text{kg}\cdot\text{kg}^{-1}$	0.75	Estimated (Human and Nicolson, 2006).
Volumetric fraction of organic matter in soil	f_{OC}	unitless	0.023	(Trapp and Matthies, 1995).
Volumetric fraction of water in soil	f_{Water}	unitless	0.35	(Trapp and Matthies, 1995).
Volumetric fraction of air in soil	f_{Air}	unitless	0.12	(Trapp et al., 2007)

Density of dry soil	$\rho_{Soil,dry}$	kg·L ⁻¹	1.6	(Trapp et al., 2007)
Density of wet soil	$\rho_{Soil,wet}$	kg·L ⁻¹	1.95	(Trapp et al., 2007)
Density of leaf	ρ_{Leaf}	kg·L ⁻¹	0.4	Estimated (Meng et al., 2021).
Density of water	ρ_{Water}	kg·L ⁻¹	1.0	Default
Density of octanol	$\rho_{Octanol}$	kg·L ⁻¹	0.83	(U.S. National Library of Medicine, 2018)
Gas conductance	g	m·d ⁻¹	86.4	(Trapp and Matthies, 1995)
Duration between insecticide application and the flowering stage	t_F	d	7	Default
Duration between insecticide application and harvest	t_H	d	50	Default (estimated according to the 6-wk flowering stage).
Elimination rate constant via dilution (plant growth)	$k_{El,Degra}$	d ⁻¹	0.035	Default value for the plant leaf (Trapp and Matthies, 1995)
Unit conversion factor 1	cf_1	mg·kg ⁻¹ per m ² ·ha	100	Calculated
Unit conversion factor 2	cf_2	L m ⁻³	1000	Calculated

S2. Insecticide dissipation kinetics in soil

The overall dissipation of the neonicotinoid insecticide from the surface soil comprises the volatilization, plant uptake, water-induced (i.e., rainfall), and degradation processes, which can be described using the first-order kinetics because the loss rates of the insecticide via these processes are proportional to the residue level in soil (Li and Niu, 2021). Thus, $k_{Diss,Soil}$ can be further expressed as follows:

$$k_{Diss,Soil} = k_{Diss,Air} + k_{Diss,Plant} + k_{Diss,Water} + k_{Diss,Deg} \quad (s14)$$

where,

$k_{Diss,Air}$ (d⁻¹) is the dissipation rate constant of the residue via volatilization;

$k_{Diss,Plant}$ (d⁻¹) is the dissipation rate constant of the residue via plant uptake;

158 $k_{Diss,Water}$ (d^{-1}) is the dissipation rate constant of the residue via surface runoff and infiltration of
159 the precipitation;

160 $k_{Diss,Deg}$ (d^{-1}) is the dissipation rate constant of the residue via degradation.

161 The estimation of rate constants for the sub-dissipation processes were taken from (Li and Niu,
162 2021). For the volatilization process, $k_{Diss,Air}$ can be estimated as follows:

$$k_{Diss,Air} = \frac{D_{Air}^0}{K_{SA} \times \rho_{Soil}^* \times d^2} \quad (s15)$$

163 where,

164 D_{Air}^0 ($m^2 d^{-1}$) is the diffusivity of the residue in gas under the reference state (298.15 K), which can
165 be estimated using the MW of the residue and the diffusivity of H₂O vapor in air (Trapp, 2007);

166 K_{SA} ($L L^{-1}$) is the partition coefficient of the residue between soil and air, which can be estimated
167 using K_{SW} and K_{AW} ;

168 ρ_{Soil}^* is the dimensionless bulk density of soil (wet);

169 d (m) is the effective diffusion length in air (i.e., air boundary layer).

170 For the plant uptake process, $k_{Diss,Plant}$ can be estimated as follows:

$$k_{Diss,Plant} = \frac{Q_{Leaf} \times LAI \times 0.001}{A_{Leaf} \times H_{Soil} \times \rho_{Soil} \times K_{SW}} \quad (s16)$$

171 For the water-induced dissipation process, $k_{Diss,Water}$ can be estimated as follows:

$$k_{Diss,Water} = \frac{I}{H_{Soil} \times \rho_{Soil} \times K_{SW}} \quad (s17)$$

172 where,

173 I ($m d^{-1}$) is the average rainfall intensity.

174 For the degradation process, $k_{Diss,Air}$ can be estimated as follows:

$$k_{Diss,Deg} = k_{Diss,Deg}^0 \times \exp \left[\frac{E_a}{R} \times \left(\frac{1}{298.15K} - \frac{1}{T_{Soil}} \right) \right] \quad (s18)$$

175 where,

176 $k_{Diss,Deg}^0$ (d^{-1}) is the degradation rate constant in the reference state (i.e., 298.15 K), which was

177 taken from the USEtox database (Fantke et al., 2017);

178 E_a ($kJ\ mol^{-1}$) is the activation energy;

179 R ($kJ\ mol^{-1}K^{-1}$) is the gas constant;

180 T_{Soil} (K) is the soil temperature.

181 The $RUD_{Soil}(0)$ value can be estimated according to Eq. (s2b) as follows:

$$RUD_{Soil}(0) = \frac{C_{Soil}(0)}{AR} = \frac{f_{Soil} \times cf_1}{\rho_{Soil} \times H_{Soil} \times cf_2} \quad (s19)$$

182 For a general estimate of the $k_{Diss,Soil}$ value of the neonicotinoid insecticide, default or generic

183 values were applied to simulate rate constants of the sub-dissipation processes, which are provided

184 in the following table.

185 Table S2. Summary of inputs of the dissipation kinetics model.

Variables	Variables	Units	Values	References
Soil temperature	T_{Soil}	K	298.15	In the reference state
Gas constant	R	$kJ\ mol^{-1}K^{-1}$	8.314	Default
Activation energy	E_a	$kJ\ mol^{-1}$	60	Default (due to information limitation) (Li and Niu, 2021).
Average rainfall intensity	I	$m\ d^{-1}$	0.0027	Default (estimated based on an average annual rainfall intensity of 1,000 $mm\ yr^{-1}$) (Li and Niu, 2021).
Effective diffusion length in air	d	m	0.01	Default (Wolters et al., 2003).

S3. Chemical-specific model inputs

The chemical-specific model inputs, including partition coefficients and rate constants, are provided in the Supplementary database. The basic physicochemical properties (e.g., K_{ow}) were taken from current studies (Fantke et al., 2017; Lewis et al., 2016).

S4. Variability analysis

S4.1 Soil properties

Soil properties have a significant impact on the estimated K_{sw} value of the insecticide residue, which further affect the simulated residue levels in plant tissues and soil. We varied soil properties shown in Table S3 to generate uncertainty intervals of K_{sw} . The selected ranges of soil properties were taken from current studies (Guo et al., 2021). The simulation results are provided in the Supplementary database.

Table S3. Selected ranges of soil properties for estimating uncertainty intervals of K_{sw} .

Input variables	Unit	Range	References
f_{oc}	g g^{-1}	0.007-0.063	(Sudduth and Hummel, 1991)
f_{water}	g g^{-1}	0.2-0.4	(Datta et al., 2008)
f_{air}	g g^{-1}	0.2-0.3	(The University of Hawaii, 2021)
$\rho_{soil,wet}$	kg L^{-1}	1.1-1.6	(Rai et al., 2017)

S4.2 Dissipation half-lives of insecticides in soil

The $k_{Diss,Soil}$ value of the insecticide is highly dependent on weather conditions (i.e., temperature and relative humidity), which further has the spatiotemporal pattern (Li and Niu, 2021). We estimated the weather-dependent $k_{Diss,Soil}$ value by investigating temperature- or humidity-based sub-dissipation processes of the residue in soil.

For the volatilization process, $k_{Diss,Air}$ is a function of T_{Air} and RH_{Air} (Davie-Martin et al., 2015, 2013), for which the full model can be found in (Li and Niu, 2021). For the plant uptake process, $k_{Diss,Plant}$ is a function of T_{Air} and RH_{Air} , for which the weather-dependent value can be estimating using Eq. (s8). For the water-induced dissipation process, $k_{Diss,Water}$ is a function of precipitation intensity, and the spatiotemporal pattern and uncertainty interval of the value can be estimated by varying the I value in Eq. (s17). For the degradation process, $k_{Diss,Air}$ is a function of T_{Soil} that has a linear relationship with T_{Air} (Islam et al., 2015).

We used annual average values to evaluate the variability and spatiotemporal pattern of the simulated RQs of neonicotinoid insecticides for honeybees and earthworms, for which the simulation results are provided in the Supplementary database.

S5. Supplementary figures

Supplementary figures are provided in this section.

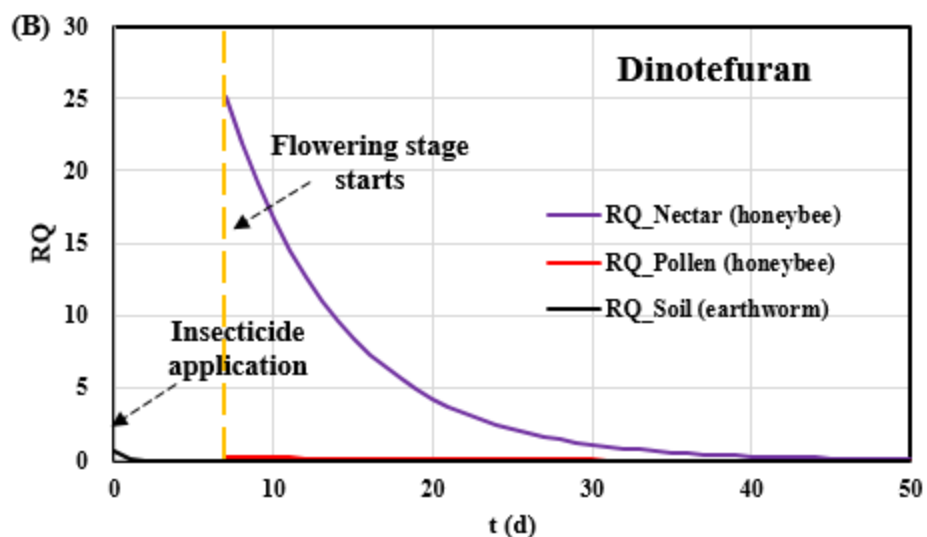
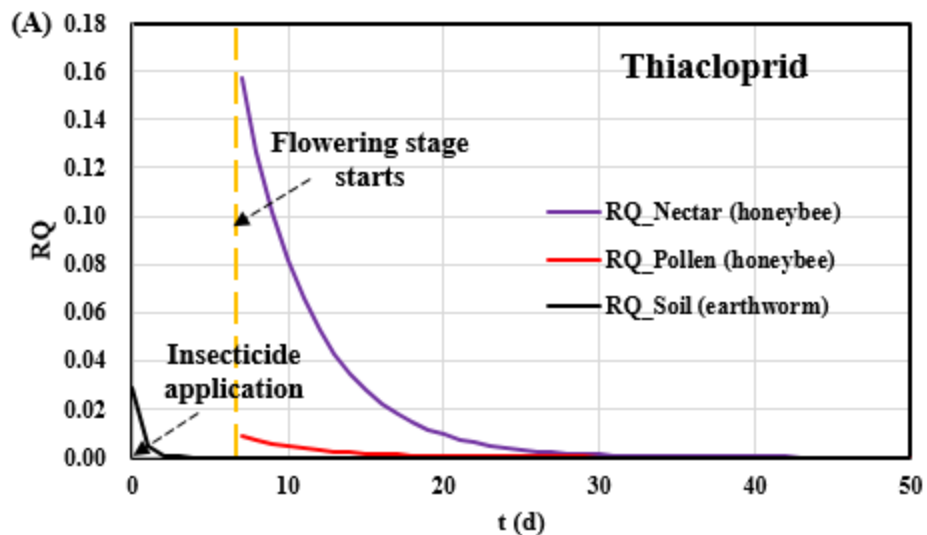


Figure S1. Simulated risk quotients (RQs) of (A) thiacloprid and (B) dinotefuran for honeybees (dietary intake of nectar and pollen) and earthworms (being exposed to soil) as functions of time (t, d) after insecticide application (t = 0). The insecticide application is assumed to occur one week before the flowering stage of the cotton plant. The RQs were simulated based on the unit application rate of the insecticide (1.0 kg ha^{-1}) to the cotton plant.

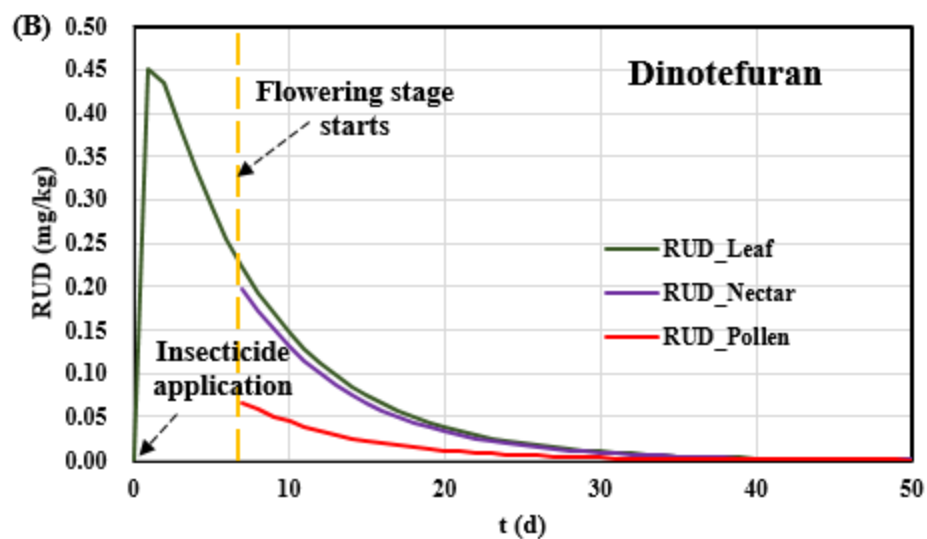
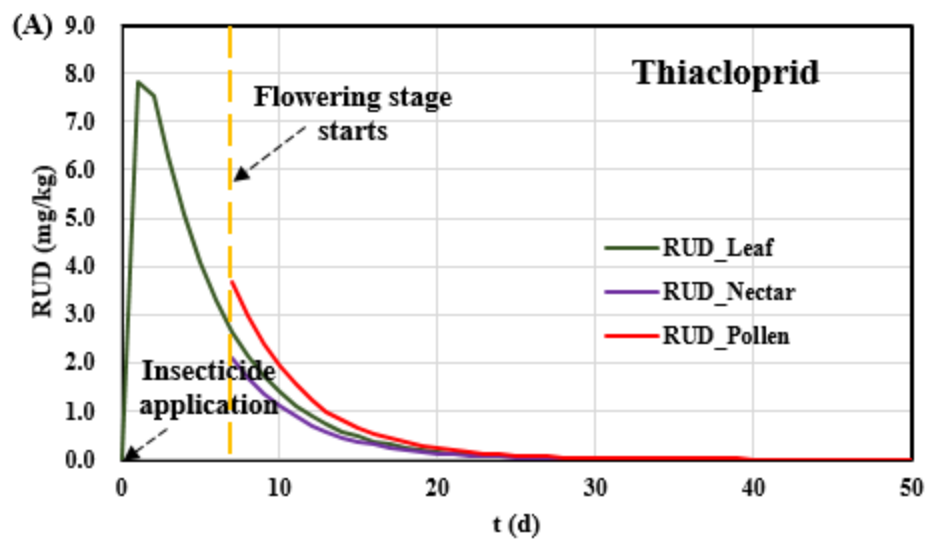
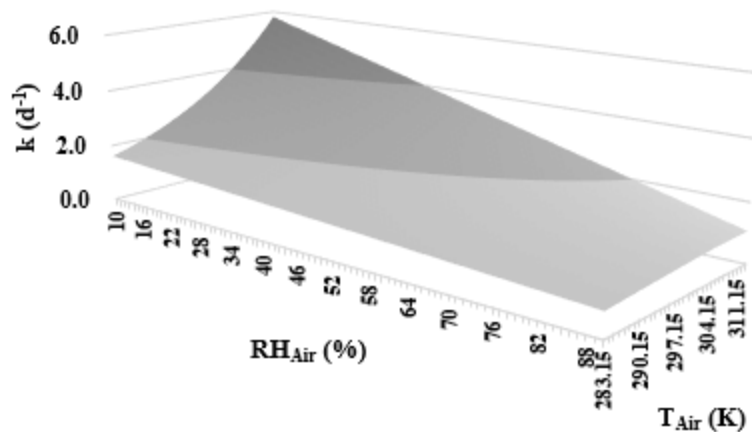


Figure S2. Simulated residue unit doses (RUDs, mg kg^{-1}) of (A) thiacloprid and (B) dinotefuran in plant tissues (leaf, nectar, and pollen) of cotton as functions of time (t , d). The insecticide application is assumed to occur one week before the flowering stage of the cotton plant.

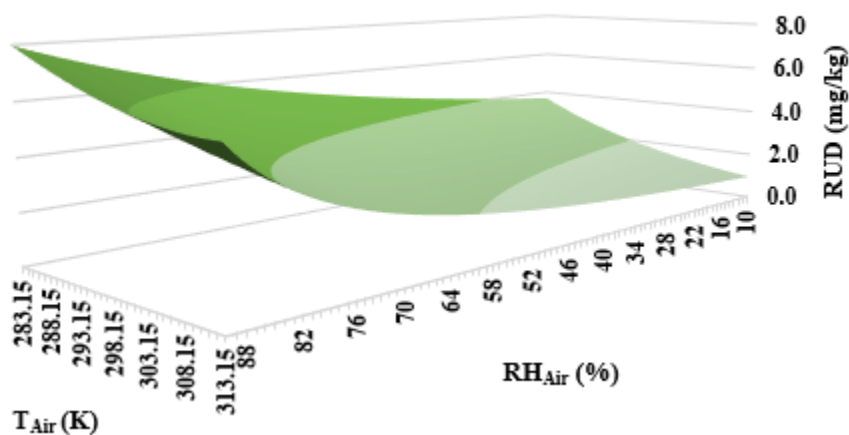
Overall dissipation rate constant in soil



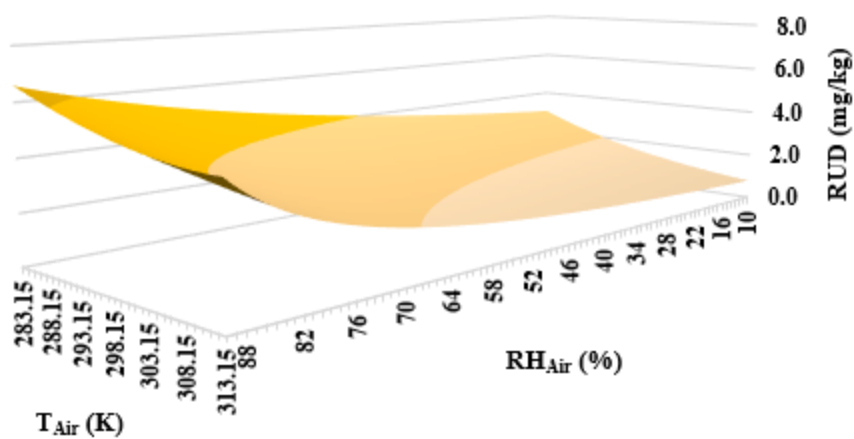
231
 232 Figure S3. Simulated overall dissipation rate constant of acetamiprid in soil ($k_{\text{Diss,Soil}}$, d^{-1}) as a
 233 function of the relative humidity of air ($RH_{\text{Air}} \in [10\%, 90\%]$) and the temperature of air ($T_{\text{Air}} \in$
 234 $[283.15\text{K}, 313.15\text{K}]$). A default value of $1,000 \text{ mm yr}^{-1}$ (0.0027 m d^{-1}) was used for the average
 235 precipitation intensity.

(A)

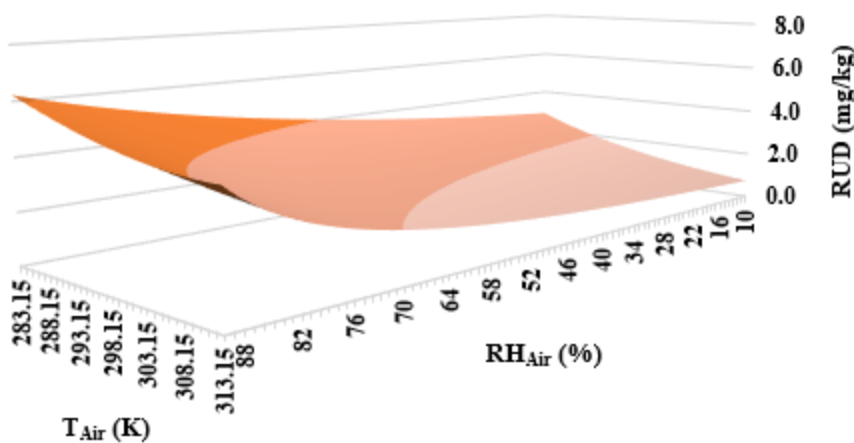
Acetamiprid in leaf



(B) Acetamiprid in nectar



(C) Acetamiprid in pollen



(D) Acetamiprid in soil

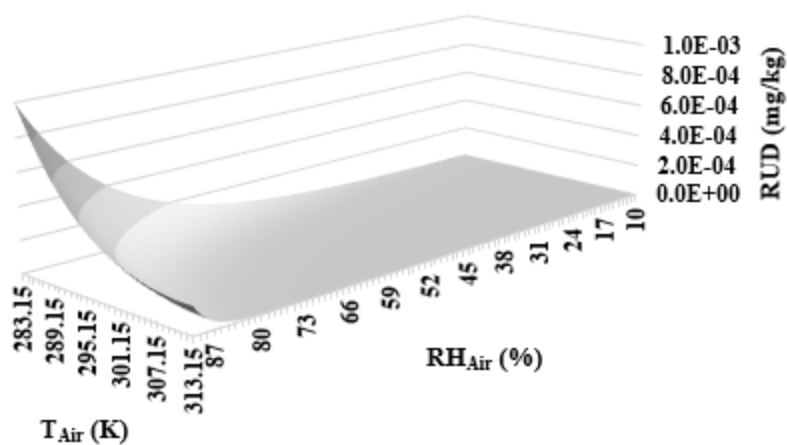


Figure S4. Simulated residue unit doses (RUDs, mg kg^{-1}) (based on the insecticide application rate of 1.0 kg ha^{-1} via foliar spray) of acetamiprid in (A) cotton leaves, (B) nectar, (C) pollen, and (D) soil as functions of the relative humidity of air ($RH_{Air} \in [10\%, 90\%]$) and the temperature of air ($T_{Air} \in [283.15\text{K}, 313.15\text{K}]$). The RUDs were simulated on 7 d after the insecticide application to the cotton plant. A default value of $1,000 \text{ mm yr}^{-1}$ (0.0027 m d^{-1}) was used for the average precipitation intensity.

S6. Model refinement for site-specific assessment

S6.1 Weather input variables

For weather conditions, users can modify the values for weather input variables (i.e., temperature, relative humidity, or rainfall intensity) in sheet "NNIs - LBs of RQs (weather)" or "NNIs - UBs of RQs (weather)" of the Supplementary Database in order to generate site-specific simulation results.

In Europe, cotton is typically grown in the south, where the average temperature during cotton-growing seasons ranges from 20°C to 30°C (i.e., from 293.15K to 303.15K). Consequently, the site-specific risk assessment for these regions of southern Europe can be conducted using the following procedures:

In the "NNIs - LBs of RQs (weather)" sheet of the Supplementary File, users can enter 293.15K in the "temperature" cell and leave other weather input variables at their default or generic values (e.g., relative humidity as 50% and rainfall intensity as 0.0027 m d^{-1}) as depicted in the screenshot below.

	X	Y	Z	AA	AB
		Tempreture	Relative humidity	Rainfall intensity	
1)	k ⁰ _{Diss,Deg}				k _{Diss,Deg}
	d ⁻¹	K	%	m/d	d ⁻¹
0	4.33E-01	293.15	50.00	2.70E-03	4.33E-01
2	1.27E-03	293.15	50.00	2.70E-03	1.27E-03
3	8.45E-03	293.15	50.00	2.70E-03	8.45E-03
0	2.24E-01	293.15	50.00	2.70E-03	2.24E-01
2	3.63E-03	293.15	50.00	2.70E-03	3.63E-03
4	7.88E-01	293.15	50.00	2.70E-03	7.87E-01
1	1.39E-02	293.15	50.00	2.70E-03	1.39E-02
UBs of Ksw		NNIs - LBs of RQs (weather)			NNIs -

Screenshot 1. Illustration of modifying weather input variables (temperature: 293.15K) for site-specific assessment.

AO	AP	AQ	AR	AS	AT	AU	AV
Aerial application					Risk assessment (based on 1 kg per ha)		
RUD _{Leaf}	RUD _{Nectar}	RUD _{Pollen}	RUD _{Soil}		RQ _{Nectar}	RQ _{Pollen}	RQ _{Soil}
mg.kg ⁻¹	mg.kg ⁻¹	mg.kg ⁻¹	mg.kg ⁻¹				
3.50E+00	2.89E+00	2.73E+00	2.31E-06		1.04E+00	3.21E-02	2.56E-06
8.89E+00	7.18E+00	7.63E+00	9.08E-05		4.76E+02	1.65E+01	6.87E-05
2.83E-01	2.53E-01	8.48E-02	4.95E-07		3.21E+01	3.50E-01	1.01E-06
3.44E-01	3.04E-01	1.14E-01	1.73E-07		8.87E-03	1.08E-04	1.73E-09
2.68E+00	2.30E+00	1.73E+00	1.28E-05		8.28E+01	2.03E+00	1.19E-05
3.06E+00	2.41E+00	4.24E+00	3.60E-06		1.81E-01	1.04E-02	3.42E-07
5.56E-01	4.90E-01	1.94E-01	9.37E-07		5.96E+01	7.68E-01	9.37E-09
..	NNIs - UBs of Ksw	NNIs - LBs of RQs (weather)			NNIs - UBs of RQs (weather)		

Screenshot 2. Illustration of simulated ecological risks by varying weather input variables (temperature: 293.15K).

The same method can be used to generate simulation results at a temperature of 303.15K.

S6.2 Exposure input variables

The operational tool proposed allows users to modify exposure input variables (i.e., honeybee daily nectar or pollen intake rates) to perform species-specific risk assessment for honeybees. The aforementioned sequential procedure can be utilized by users to conduct the simulation. Users can modify the numeric values in the mathematical formulas of the cells "RQ Nectar" and "RQ Pollen" to determine their specific honeybee daily nectar and pollen consumption rates, respectively. The simulation process is depicted in the diagram below.

275 If the nectar consumption rate is set to 40 mg/bee/d (i.e., 0.00004 kg/bee/d) rather than 292
 276 mg/bee/d (i.e., 0.000292 kg/bee/d) as stated in the main text, then users can enter the numeric value
 277 0.00004 in the mathematical formula of the cell "RQ Nectar" in the sheet "NNIs - default values"
 278 (or any calculation sheet), as shown in the screenshot below.

279

	C	D	AP	AQ
				Risk assessment
a	LD ₅₀ - oral (mg bee)	LD ₅₀ - earthworms		RQ _{Nectar}
iprid	8.09E-03	9		C6/10

280 Screenshot 3. Illustration of modifying exposure input variables for site-specific assessment.

281 Then, users can obtain the simulated ecological risks (i.e., RQ Nectar) corresponding to the
 282 modified nectar consumption rates, as depicted in the following screenshot.

283

	AQ	AR	AS	AT
	Risk assessment (based on 1 kg per ha)			
	RQ _{Nectar}	RQ _{Pollens}	RQ _{Soil}	
	1.18E-01	2.65E-02	2.71E-07	
	5.12E+01	1.29E+01	8.58E-06	
	3.44E+00	2.74E-01	3.34E-08	
	9.68E-04	8.64E-05	6.41E-11	
	8.78E+00	1.57E+00	9.05E-07	
	2.16E-02	9.01E-03	7.67E-08	
	6.35E+00	5.97E-01	3.69E-10	

Screenshot 4. Illustration of simulated ecological risks by modifying exposure input variables.

S6.3 Toxicological input variables

In this study, a 10 uncertainty factor was used to account for inter- or intra-species variability; however, this value may be an overestimate or underestimate of the actual toxicity of pesticides to non-target organisms. In order to conduct a more accurate assessment of the ecological risk, the toxicological data should be updated. Users can modify the uncertainty factor and toxicological data for honeybees or earthworms in the spreadsheet. As shown in the screenshot below, users can enter an uncertainty factor of 5, rather than 10, in the mathematical formula tabulated for the cell "RQ."

=A06/(D6/5)						
	C	D	AP	AQ	AR	AS
				Risk assessment (based on 1 kg per ha)		
	LD ₅₀ – oral (mg bee ⁻¹)	LC ₅₀ – earthworms (mg a.i. ⁻¹)		RQ _{Nectar}	RQ _{Pollen}	RQ _{Soil}
imid	8.09E-03	9		1.18E-01	2.65E-02	5)
idin	4.40E-05	13.21		5.12E+01	1.29E+01	8.58E-06
ran	2.30E-05	4.9		3.44E+00	2.74E-01	3.34E-08
mid	1.00E-01	1000		9.68E-04	8.64E-05	6.41E-11

Screenshot 5. Illustration of modifying toxicological input variables for species-specific risk assessment.

297 **References**

- 298 Chiou, C.T., Sheng, G., Manes, M., 2001. A partition-limited model for the plant uptake of organic
299 contaminants from soil and water. *Environmental Science and Technology*.
300 <https://doi.org/10.1021/es0017561>
- 301 Datta, S., Taghvaeian, S., Stivers, J., 2008. Understanding Soil Water Content and Thresholds for
302 Irrigation Management [WWW Document]. URL [https://extension.okstate.edu/fact-](https://extension.okstate.edu/fact-sheets/understanding-soil-water-content-and-thresholds-for-irrigation-management.html)
303 [sheets/understanding-soil-water-content-and-thresholds-for-irrigation-management.html](https://extension.okstate.edu/fact-sheets/understanding-soil-water-content-and-thresholds-for-irrigation-management.html) (accessed
304 5.26.21).
- 305 Davie-Martin, C.L., Hageman, K.J., Chin, Y.P., 2013. An improved screening tool for predicting
306 volatilization of pesticides applied to soils. *Environmental Science and Technology*.
307 <https://doi.org/10.1021/es3020277>
- 308 Davie-Martin, C.L., Hageman, K.J., Chin, Y.P., Rougé, V., Fujita, Y., 2015. Influence of Temperature,
309 Relative Humidity, and Soil Properties on the Soil-Air Partitioning of Semivolatile Pesticides:
310 Laboratory Measurements and Predictive Models. *Environmental Science and Technology*.
311 <https://doi.org/10.1021/acs.est.5b02525>
- 312 Fantke, P., Charles, R., Alencastro, L.F. de, Friedrich, R., Jolliet, O., 2011. Plant uptake of pesticides and
313 human health: Dynamic modeling of residues in wheat and ingestion intake. *Chemosphere*.
314 <https://doi.org/10.1016/j.chemosphere.2011.08.030>
- 315 Fantke, P. (Ed.), Bijster, M., Guignard, C., Hauschild, M., Huijbregts, M., Jolliet, O., Kounina, A.,
316 Magaud, V., Margni, M., McKone, T.E., Posthuma, L., Rosenbaum, R.K., van de Meent, D., van
317 Zelm, R., 2017. USEtox® 2.0 Documentation (Version 1).
- 318 Guo, Y., Xiao, S., Li, Z., 2021. A screening model for managing periodic pesticide application in
319 residential lawn soils. *Environmental Advances*. <https://doi.org/10.1016/j.envadv.2021.100078>
- 320 Human, H., Nicolson, S.W., 2006. Nutritional content of fresh, bee-collected and stored pollen of *Aloe*
321 *greatheadii* var. *davyana* (Asphodelaceae). *Phytochemistry* 67.
322 <https://doi.org/10.1016/j.phytochem.2006.05.023>
- 323 Islam, K.I., Khan, A., Islam, T., 2015. Correlation between Atmospheric Temperature and Soil
324 Temperature: A Case Study for Dhaka, Bangladesh. *Atmospheric and Climate Sciences*.
325 <https://doi.org/10.4236/acs.2015.53014>
- 326 Juraske, R., Antón, A., Castells, F., 2008. Estimating half-lives of pesticides in/on vegetation for use in
327 multimedia fate and exposure models. *Chemosphere*.
328 <https://doi.org/10.1016/j.chemosphere.2007.08.047>
- 329 Juraske, R., Antón, A., Castells, F., Huijbregts, M.A.J., 2007. Human intake fractions of pesticides via
330 greenhouse tomato consumption: Comparing model estimates with measurements for Captan.
331 *Chemosphere*. <https://doi.org/10.1016/j.chemosphere.2006.11.047>
- 332 Lewis, K.A., Tzilivakis, J., Warner, D.J., Green, A., 2016. An international database for pesticide risk
333 assessments and management. *Human and Ecological Risk Assessment*.
334 <https://doi.org/10.1080/10807039.2015.1133242>

Li, Z., 2022. Modeling pesticide residues in nectar and pollen in support of pesticide exposure assessment for honeybees: A generic modeling approach. *Ecotoxicology and Environmental Safety* Accepted.

Li, Z., 2021. Approximate Modeling of the Uptake of Pesticides by Grass for Grazing Risk Assessment and Pasture Management. *ACS Agricultural Science & Technology*.
<https://doi.org/10.1021/acsagscitech.1c00036>

Li, Z., 2020. Spatiotemporal pattern models for bioaccumulation of pesticides in common herbaceous and woody plants. *Journal of Environmental Management*.
<https://doi.org/10.1016/j.jenvman.2020.111334>

Li, Z., Niu, S., 2021. Modeling pesticides in global surface soils: Evaluating spatiotemporal patterns for USEtox-based steady-state concentrations. *Science of The Total Environment* 791.
<https://doi.org/10.1016/j.scitotenv.2021.148412>

Meng, H., Lei, Z., Zhang, W., Zhang, Y., 2021. Variation mechanism of leaf mass per area in cotton under the systematic regulation. *Cotton Science* 33, 144–154.

Monteiro, J.B.E.A., Sentelhas, P.C., Chiavegato, E.J., 2006. Microclimate and ramulosis occurrence in a cotton crop under three plant population densities in southern Brazil. *AgriScientia* 23.
<https://doi.org/10.31047/1668.298x.v23.n2.2691>

Mukherjee, T., Ivanova, M., Dagda, M., Kanayama, Y., Granot, D., Holaday, A.S., 2015. Constitutively overexpressing a tomato fructokinase gene (LeFRK1) in cotton (*Gossypium hirsutum* L. cv. Coker 312) positively affects plant vegetative growth, boll number and seed cotton yield. *Functional Plant Biology* 42. <https://doi.org/10.1071/FP15035>

Paraíba, L.C., Katagiri, K., 2008. Model approach for estimating potato pesticide bioconcentration factor. *Chemosphere*. <https://doi.org/10.1016/j.chemosphere.2008.07.026>

Rai, R.K., Singh, V.P., Upadhyay, A., 2017. Chapter 17 - Soil Analysis, in: *Planning and Evaluation of Irrigation Projects*.

Sudduth, K.A., Hummel, J.W., 1991. EVALUATION OF REFLECTANCE METHODS FOR SOIL ORGANIC MATTER SENSING. *Transactions of the ASAE* 34, 1900–1909.

The University of Hawaii, 2021. Soil Composition [WWW Document]. URL https://www.ctahr.hawaii.edu/mauisoil/a_comp.aspx (accessed 5.26.21).

Trapp, S., 2007. Fruit tree model for uptake of organic compounds from soil and air. SAR and QSAR in Environmental Research. <https://doi.org/10.1080/10629360701303693>

Trapp, S., Cammarano, A., Capri, E., Reichenberg, F., Mayer, P., 2007. Diffusion of PAH in potato and carrot slices and application for a potato model. *Environmental Science and Technology*.
<https://doi.org/10.1021/es062418o>

Trapp, S., Matthies, M., 1995. Generic One-Compartment Model for Uptake of Organic Chemicals by Foliar Vegetation. *Environmental Science and Technology*. <https://doi.org/10.1021/es00009a027>

U.S. National Library of Medicine, 2018. National Center for Biotechnology Information - Chemicals & Bioassays [WWW Document].

372 Wilson, J.R., Mannetje, L., 1978. Senescence, digestibility and carbohydrate content of buffel grass and
373 green panic leaves in swards. Australian Journal of Agricultural Research 29.
374 <https://doi.org/10.1071/AR9780503>

375 Wolters, A., Linnemann, V., Herbst, M., Klein, M., Schäffer, A., Vereecken, H., 2003. Pesticide
376 volatilization from soil: Lysimeter measurements versus predictions of European registration
377 models. Journal of Environmental Quality. <https://doi.org/10.2134/jeq2003.1183>

378